Textile-Based Pressure Sensors for Monitoring Prosthetic-Socket Interfaces

Jordan Tabor, Talha Agcayazi, Aaron Fleming, Brendan Thompson, Ashish Kapoor, Ming Liu, *Member, IEEE*, Michael Y. Lee, He Huang, *Senior Member, IEEE*, Alper Bozkurt, *Senior Member, IEEE*, and Tushar K. Ghosh, *Member, IEEE*

***Abstract*—Amputees are prone to experiencing discomfort when wearing their prosthetic devices. As the amputee population grows this becomes a more prevalent and pressing concern. There is a need for new prosthetic technologies to construct more comfortable and well-fitted liners and sockets. One of the well-recognized impediments to the development of new prosthetic technology is the lack of practical inner socket sensors to monitor the inner socket environment (ISE), or the region between the residual limb and the socket. Here we present a capacitive pressure sensor fabricated through a simple, and scalable sewing process using commercially available conductive yarns and textile materials. This fully-textile sensor provides a soft, flexible, and comfortable sensing system for monitoring the ISE. We provide details of our low-power sensor system capable of high-speed data collection from up to four sensor arrays. Additionally, we demonstrate two custom set-ups to test and validate the textile-based sensors in a simulated prosthetic environment. Finally, we utilize the textile-based sensors to study the ISE of a bilateral transtibial amputee. Results indicate that the textile-based sensors provide a promising potential for seamlessly monitoring the ISE.**

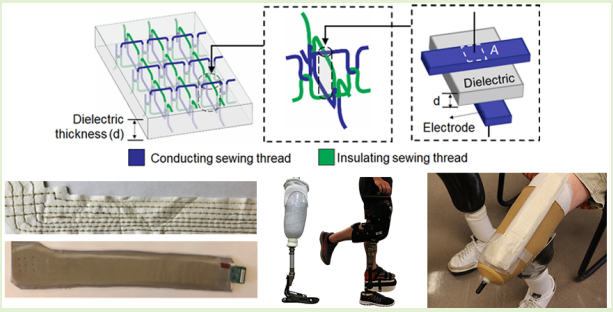

***Index Terms*—Pressure sensors, capacitive sensors, sensor arrays, body system networks, sensor systems and applications, textiles, wearable sensors, flexible electronics, prosthetics.**

I. Introduction

AMPUTATION is one of the major causes of disability with approximately 1.7 million people living with limb loss in the U.S. alone [1]. The majority of amputees express low satisfaction with their prosthetic devices [2], [3] as well as moderate to severe pain when wearing their prosthetic devices [3]–[5]. While wearing a prosthesis, an amputee's residual limb is exposed to an uncomfortable environment within the socket, including high stress [2], [5], which can cause debilitating pressure ulcers [6], may require further amputation [7], or result in life-threatening deep tissue injuries [6]. In fact, skin lesions occur in ∼60% of lower limb (LL) amputees resulting ∼25% of amputees reducing the use of their prosthetic [8]. One of the main hurdles in the development of new and improved prosthetic technologies is the lack of practical pressure sensors for monitoring the inner socket environment (ISE) [9].

Reported clinical studies on pressure distribution within the ISE primarily employed commercially available, rigid strain gauge sensors [10]–[13]. While these sensors provide valuable information regarding the ISE, they are disadvantageous due to their bulkiness [14], weight [15], [16], inflexibility [15], [16], low spatial resolution [17], cost [18], [19], and laborious integration methods outside of the socket [20]. Newly commercialized, semi-flexible pressure monitoring systems such as the Pliance® system (Novel® GMBH, Germany) [21], [22], or the F-Socket® (Tekscan, Inc. USA) [7], [23] have also been used to measure the pressure within the ISE. While these systems do not require socket modification, they are still spatially limited, cannot be readily integrated into

Manuscript received November 19, 2020; revised January 2, 2021; accepted January 7, 2021. Date of publication January 21, 2021; date of current version March 5, 2021. This work was supported in part by the North Carolina State University (NCSU) Chancellor's Innovation Fund, in part by NCSU Provost Fellowship, in part by NSF Electrical, Communications and Cyber Systems (ECCS) under Grant 1509043, in part by NSF Smart and Connected Health (SCH) under Grant 1622451, in part by NSF Graduate Research Fellowship under DGE-1252376, in part by the Advanced Self-Powered Systems of Integrated Sensors and Technologies Engineering Research Center (ASSIST ERC) under Grant EEC-1160483, and in part by the National Institutes of Health (NIH) under Grant NIH NICHD F31HD101285. The associate editor coordinating the review of this article and approving it for publication was Dr. Edward Sazonov. *(Jordan Tabor and Talha Agcayazi contributed equally to this work.) (Corresponding authors: Alper Bozkurt; Tushar K. Ghosh.)*

Jordan Tabor, Ashish Kapoor, and Tushar K. Ghosh are with the Department of Textile Engineering, Chemistry, and Science, North Carolina (NC) State University, Raleigh, NC 27695 USA (e-mail: tghosh@ncsu.edu).

Talha Agcayazi was with the Electrical and Computer Engineering Department, North Carolina State University, Raleigh, NC 27606 USA. He is now with Facebook, Inc., Menlo Park, CA 98022 USA.

Aaron Fleming, Ming Liu, and He Huang are with the Department of Biomedical Engineering, North Carolina (NC) State University, Raleigh, NC 27695 USA.

Brendan Thompson and Alper Bozkurt are with the Department of Electrical and Computer Engineering, North Carolina (NC) State University, Raleigh, NC 27695 USA (e-mail: aybozkur@ncsu.edu).

Michael Y. Lee is with the Baylor College of Medicine, Houston, TX 77030 USA.

Digital Object Identifier 10.1109/JSEN.2021.3053434

existing prosthetic components, and leave room for improvement in flexibility and breathability desirable for long-term use. More recently, new research-grade sensors for monitoring pressure within the ISE have been proposed in the literature. These include a MEMS-based bubble sensor [24], custom socket inserts with embedded commercial force-sensing resistors [25], and sensors fabricated via 3D printing/lithography [6], [26]. However, these proposed sensors contain rigid components [20], [24], [25], [27]–[29], require socket modification [27]–[29], are fabricated through complex and costly methods [6], [25], [26], [30], and have not been tested in-vivo [24], [27].

Some of the shortcomings associated with currently available pressure monitoring systems could be significantly improved using textile-based sensors. These sensors present obvious advantages due to their compliant and breathable nature [31] as well as their potential manufacturing using relatively simple fabrication methods. Further, textile-based sensors provide opportunities for large-area sensing and unobtrusive pressure-mapping of the entire residual limb by integrating sensors into existing and conventional textile-based components of the prosthetic system such as liner-liners and socks worn under rigid prosthetic devices. Textile-based sensors have been explored for monitoring various stimuli, most commonly, pressure [32]–[34] or strain [35]–[37] in various applications; however, their potential for monitoring pressure within the ISE has not yet been demonstrated. Here, we present a fully-textile sensor system for monitoring pressure within the ISE. The system consists of a network of capacitive sensors formed using appropriately sewn conductive and insulating threads on a textile substrate. The sewing threads, subsequently referred to as "seam-lines," form the electrodes and the textile substrate acts as the dielectric. The custom low-power electronic readout system attached to the textile sensing elements is capable of high-speed data collection from up to four sensor arrays. Previously, we demonstrated the seam-line pressure sensing approach for planar interfaces via benchtop experiments [38]–[41]. In this work, we evaluate a set of new seam-line sensors (SLS) and corresponding custom-designed electronics for ISE pressure monitoring. The SLS evaluation is performed on curved surfaces during dynamic experiments to systematically work towards our final goal of monitoring the ISE. We report two preliminary experiments: first, evaluating the sensors on an artificial limb followed by human testing with an able-bodied subject donning a bent-knee adapter to replicate the ISE. Following the preliminary experimentation, we complete an in-vivo proof-of-concept study with a bilateral transtibial amputee. The SLS successfully detected pressure changes within the ISE during weight-shifting and walking trials. Results indicate that the SLS may provide a promising approach to monitoring the pressure distribution within the ISE.

II. System Design

The sensing system comprises three parts: a sensor array, a miniature printed circuit board (PCB) adjacent to the sensors for analog to digital conversion (ADC), and a data collection PCB. The prototype system allows for data collection from four sensor arrays each consisting of nine capacitive sensors, which we refer to as textile sensing elements, or "texels". The system offers both wireless Bluetooth Low Energy or wired USB data transmission and an optional onboard data collection on a micro-SD card. Other features of this custom system include: (1) texel interconnects that reduce encumbrance and improve flexibility (see Figure 1b), (2) novel thread to PCB connections (see Figure 1b), (3) active electric field shielding around the sensor arrays and interconnects to diminish electric field noise (see Figure 1c), (4) the ADC PCB digitizing the analog sensor readouts before transmission to avoid interference noise (see Figure 1b), (5) parallel sensor array for increased spatial sampling rates, (6) low power consumption allowing up to twelve hours of data collection with a small lithium polymer battery, (7) trigger channel to synchronize the system time with external data collection systems, and (8) a real-time data visualization software for rapid sensor validation. Further details of these features will be provided subsequently.

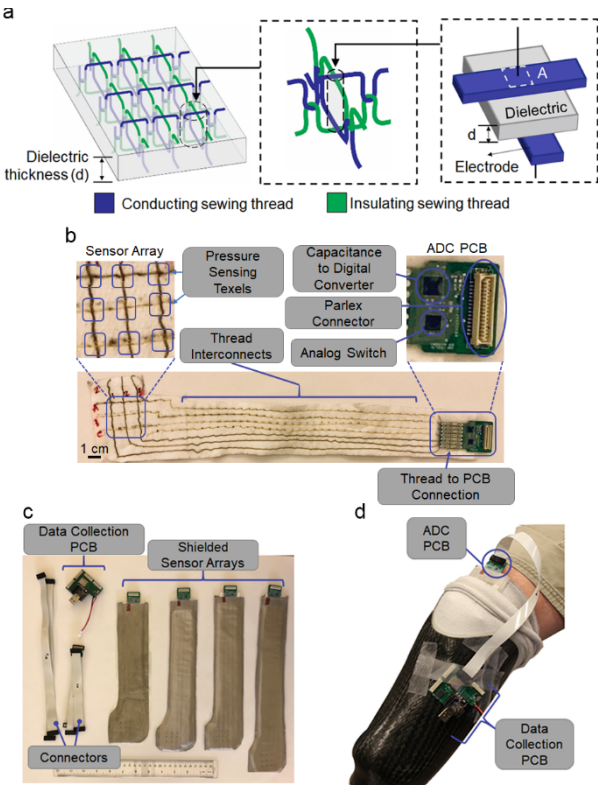

Fig. 1. Sensor architecture, system design, and integration (a) Schematic of fabric-based sensor array, showing fabric/thread-based parallel plate capacitor (figure adapted form [41]) (b) Sensor arrays, interconnects, and ADC PCB (c) Data collection PCB with four shielded sensor arrays (d) SLS sensor placed within the ISE beneath the sock with the ADC PCB attached. The ADC PCB of each sensor is connected to the exterior data collection system using flexible cables. The data collection PCB is mounted to the exterior socket to minimize encumbrance.

A. Sensor Array

The sensor architecture used in this work consists of a network of texels formed through perpendicularly sewn seam-lines, using conductive and insulating yarns, on a com-

mercial sewing machine (Durkopp E901/6, Duerkopp-Adler AG, Germany) to create 3 × 3 sensing arrays (see Figure 1a) [41]. The capacitive response of our sensor can be modeled by a parallel plate capacitor with conductive yarns serving as electrodes and the textile material as the dielectric, as shown in Figure 1a. The capacitance, C, is defined using vacuum permittivity ε_0, dielectric constant ε_r, area of the conductive electrodes A, and the distance between the conductive electrodes d,as $C = \varepsilon_O \varepsilon_r (\frac{A}{d})$. The sensed change in capacitance, $\Delta C = C_P - C_O$, results from a change in d and possibly in ε_r and A, due to applied pressure. Here, C_0 and C_p are the capacitance values before and after the application of pressure, respectively.

An advantage of the SLS fabrication method is the tunability of the sensor design. The spatial resolution, or the density of the sensing points, can be easily altered within a large range. Here, texels were placed 1 cm apart but, this could easily be changed by altering the stitch length and proximity of the seamlines for the application requirements. Additionally, the size of the array (number of texels) can be easily increased by adding additional seamlines but is limited by the electrical conductivity of the electrode materials. Further, the mechanical and sensing properties of the SLS can be tuned by proper selection of the textile dielectric. For example, the magnitude of the force that can be measured by the SLS primarily depends on the compressive properties of the dielectric thus providing desirable design flexibility.

The textile dielectric used in this research is a melt-blown fabric having a thickness of 1.82 ± 0.05 mm and comprised of a styrene-ethylene-butylene-styrene (SEBS) linear triblock copolymer material (Kraton™ MD 1653, Kraton Corp.) [41]. SEBS was chosen for its mechanical and dielectric behavior including low baseline shifts and low sensitivity to moisture (moisture regain of 0.72 ± 0.01%), necessary for pressure sensing within the ISE [41]. The conductive sewing thread used as electrodes is a commercially available silver-coated polyamide 6,6 yarn (Shieldex 235/36 4 ply, V Technical Textiles, Inc., USA) with a diameter of 468.186 ± 114.206 μm and having electrical resistance of 0.29 ± 0.033 Ω/cm [41].

The sensor arrays are designed to measure the pressure at specific lower-limb anatomical locations which could be up to 30 cm inside the socket. To place the sensors inside the socket while minimizing encumbrance, we used the same thread and dielectric material for sensor fabrication and sensor interconnect (see Figure 1b). Therefore, the interconnect possessed the same thickness and compliance as the sensor, without creating extra discomfort for the user. Additionally, a grounding thread was sewn between the row and column threads to reduce crosstalk and capacitance between the closest row/column threads.

To remove the effects of environmental electromagnetic noise on the sensor, we formed a Faraday cage around the entire sensor assembly, including the textile−PCB connections with a commercial conductive copper-nickel coated polyester fabric (Titan RF Faraday Fabric, MOS Equipment, Inc., USA) as seen in Figure 1c. The conductive fabric was attached to the sensor using double-sided adhesive tape (Scotch 34-8517-0998-9, 3M Ltd, USA).

B. Analog to Digital Conversion Printed Circuit Board

As mentioned earlier, the ADC PCB is a custom-designed board for converting the capacitance of the sensor array to digital signals for a reliable RF interference-resilient transmission. The ADC PCB was placed outside the socket at the end of the thread interconnects, as close to the sensor as possible to reduce the effects of electromagnetic noise (see Figure 1d). The flexible thread to the rigid PCB connections was achieved using vias for alignment and connection pads covered with Z-axis tape (9703, 3M Ltd, USA) for robust electrical connections. The main components of the PCB included a capacitance to digital converter with a built-in multiplexer (AD7142, Analog Devices Inc, USA) and a quad analog switch (ADG788, Analog Devices Inc, USA) for row selection. Aside from the address select resistors, the ADC PCB design was the same for each sensor array.

C. Data Collection Printed Circuit Board

The data collection PCB is a custom-designed board for collecting the digitized capacitance values from four ADC PCBs and storing/transmitting the data. This PCB contains a Bluetooth enabled microcontroller module (RFD77001, Simblee, USA), micro-SD card socket, synchronization connector, and a UART connector. Another reason for having external ADC boards was to increase the sampling rate by parallelizing the data collection routine. This enabled us to achieve a 20 Hz sampling rate with four sensor arrays which was four times faster than a sequential data collection method. We selected the current sampling rate based on the optimal performance of our electronics. To our knowledge, no study has reported the sampling rate required to capture the dynamics of inner socket pressure changes during walking or other locomotive tasks. The most relevant publication reports that a 100 Hz frequency is required for measuring plantar pressure during walking [42] However, our goal within this study was to determine whether the sensed pressure aligned with the expectation during each demonstration (e.g. higher pressure was expected in the stance than the swing phase of gait), rather than to capture the dynamics of pressure during activity. For this application, the used sampling rate was adequate. In the future, we plan to increase the sampling rate to at least 100 Hz and study the frequency components of the sensed inner socket pressure during various locomotor conditions (e.g. speed and terrain).

We performed a power consumption analysis of our system at the fastest sampling rate. The current draw breakdown was measured to be 1.2 mA for each sensor array and 6 mA for the rest of the system excluding the SD card. With four sensor arrays and an SD card, the current consumption was 40.8mA (including the typical 30mA power consumption of the SD card). This means that with a small-sized 500mAh Lithium Polymer battery, the entire system could collect data for approximately twelve hours before needing to be recharged. To limit packet loss, all experimental data reported in this article was collected with a USB connection. The data collection board is shown in Figure 1c and d.

D. Real-Time Data Visualization

During our experiments, we found that real-time data visualization was a significant factor for rapidly verifying sensors before experiments. For this, we composed a MATLAB (MathWorks Inc, USA) code to receive and plot the transmitted capacitance values in real-time. Sensors were tested using this real-time data visualization routine before and after experimentation to double-check their successful operation. This validation step allowed us to visually inspect the sensor response to mechanical stimulus and identify any potential failure modes before lengthy experiments.

III. Sensor Evaluation in Simulated Inner Socket Environment

To adequately prepare for in-vivo assessment of the efficacy of our textile-based sensors to monitor the ISE, we conducted two preliminary evaluations. This included the use of an artificial limb simulating potential inner-socket pressure ranges [43] and an able-bodied subject walking with a bent-knee adapter for gait patterns that could occur during amputee locomotion [44], [45]. These setups allowed for an intermediate well-controlled environment for testing. All the presented human experimentation was performed with the approval of the Institutional Review Board at the University of North Carolina at Chapel Hill where the study participants were provided informed, written consent to participate.

We would like to emphasize that the full calibration of the sensor response (conversion of capacitance to absolute pressure) is currently beyond the scope of this article and reserved for a follow up future study involving a more detailed evaluation. Full calibration of the SLS requires quantitative measurement of the output of each group of texels (depending on the necessary spatial resolution) at the beginning of each use, because of the unique initial shape of the sensor array (curvature, etc.) and time-dependent change of its mechanical behavior. This will be the subject of continuing research and future publications in the development of the SLS. Therefore, here, we report relative capacitive changes to provide a valuable qualitative understanding of the ISE, such as relative pressure changes with activity and relative differences in pressure at various locations. For a more comprehensive understanding of individual texel's sensory behavior, we refer the interested reader to our previous publication [41].

A. Artificial Limb Testing

In the first simulated ISE experiment, we used a custom artificial limb secured to a frame (see Figure 2a and b). The limb was tilted to predetermined angles and then screwed in place on the frame to induce different loading patterns on the SLS. The main objective of this experiment was to measure the sensor response (ΔC) at certain regions of the limb given a change in pressure due to different angles of tilt. Capacitance changes were measured at angles ranging from $-15°$ (Left-side position 5 (L5)) to $+9°$ (Right-side position 3 (R3)) as shown in Figure 2b. Measurements were taken at increments of 3° (i.e., L5 corresponded to $-15°$, L4 to $-12°$, L3 to $-9°$, L0/R0 (Neutral) to 0°, R1 to $+3$, and so on).

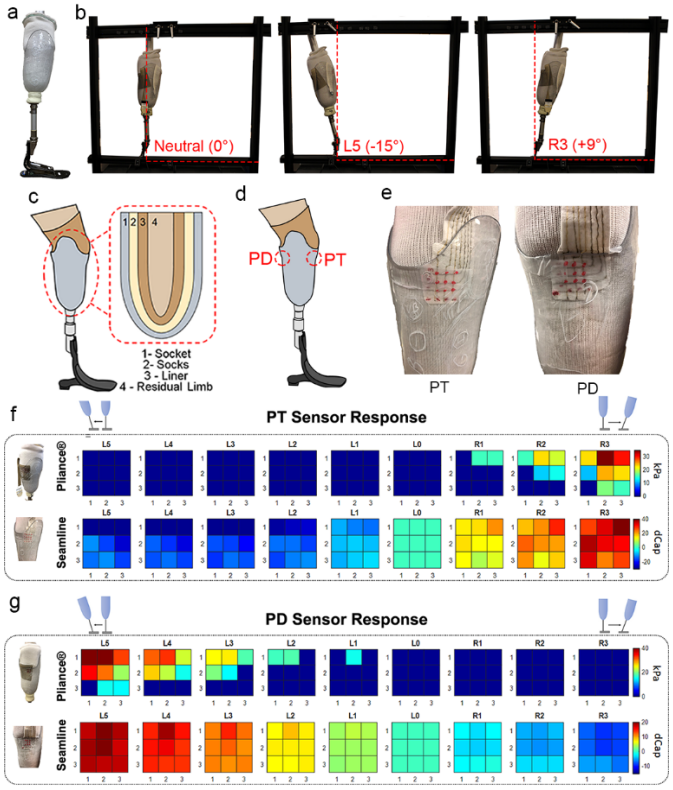

Fig. 2. Artificial limb testing set-up and results (a) Artificial limb (b) Artificial limb on supporting frame at neutral, L5, and R3 positions (c) Diagram of artificial limb prosthetic components (d) Positions of sensor placement (e) Placement of SLS on the PT and PD. Comparative results of pressure distribution from nine sensing points (3×3) of the Pliance® and seam-line sensor arrays placed at the (f) PT, and (g) PD. The baseline capacitance data for the SLS at the neutral position was removed from the capacitance recordings. The Pliance® sensor is unable to detect pressures $<$15kPa, and therefore some sensing points showed no response throughout the experiment.

The custom transtibial artificial limb and corresponding socket were fabricated by a prosthetist. The artificial residual limb was made using a commercial plaster (Gold Bond Brand Super White Moulding Plaster, National Gypsum LLC, USA) while the socket was fabricated using a transparent co-polyester material (Vivak®, Plaskolite LLC, USA) commonly used for test sockets. The socket was transparent which allowed us to easily align and monitor the sensors during the experiments. The plaster-socket interface contained a silicone liner and three textile socks which were removable to create more space inside the interface (see Figure 2c).

During these preliminary experiments, unshielded sensors were placed on two areas of clinical interest where prosthetic sockets typically apply higher levels of pressure: the patella tendon (PT) (i.e. anterior location) and popliteal depression (PD) (i.e. posterior location) [13], [22] (see Figure 2d). To find specific regions of interest within these areas (i.e., areas with a detectable change in pressure due to changes in the angle of tilt) we used a commercial pressure sensing array: the Pliance® system (Pliance® Hand/palm Elastic Sensor ES-FE-64-EL10, Novel® GmbH, Germany). The commercial sensor array was placed on several positions along with the PT and PD and the limb was tilted – regions of the PT and PD with distinct pressure changes were selected for the formal study. Specifically,

nine of the sixty-four Pliance® sensing points were selected and marked on the transparent socket in red ink such that the nine texels of the SLS could be placed in the same location (see Figure 2e). The pressure measurements recorded using the Pliance® system were used to qualitatively compare with those from our sensor.

The resulting data from the Pliance® sensor and the SLS are plotted as heatmaps for comparison in Figure 2f and g. As expected, when the limb was tilted forward, toward position R3, the sensor output (ΔC) increased for the sensor located on the anterior of the artificial limb (i.e. PT location). Conversely, when considering the posterior sensor placement (i.e., PD location), the output signal increased when the limb was tilted backward, or towards L5, and decreased when tilted forward. It is important to note that the Pliance® sensor is unable to detect pressures $<$15kPa, and therefore some sensing points showed no response throughout the experiment. In general, the pressure gradient across the Pliance® and SLS sensor arrays were similar across the tilt angles tested. This means that the SLS could be used as a pressure sensor to track the relative change in the distribution of forces. The SLS also seems to be more sensitive in the smaller pressure ranges, which might be desirable for sensitive anatomical regions in the socket-limb interface.

B. Able-Bodied Testing With Bent-Knee Adapter

Following the evaluation of the SLS using the artificial limb set-up, we tested the sensors using a custom-made bent-knee adapter as shown in Figures 3a and 3b. The bent-knee adapter provides a useful intermediate step between artificial limb testing and in-vivo amputee testing; it is a physical interface between human soft tissues and rigid material, which simulates the socket interface. Able-bodied studies also help determine if the sensors and the corresponding electronics are sufficiently durable to withstand in-vivo testing (weight shifting and walking) before recruiting an amputee participant. Further, using a healthy subject during this intermediate evaluation poses fewer risks and burdens to amputee subjects who may be suffering from comorbidities which can hinder extended periods of standing and walking during testing.

The healthy participant wore a modified prosthetic liner such that the interface environment was more realistic and a single unshielded SLS was attached outside the liner during testing with medical wrap, as shown in Figure 3c. Similar to the artificial limb experiments, we used the commercial Pliance® pressure sensor to identify a general region of interest, specifically, a region where the pressure distribution among nine sensing points was notable while the pressure changes with the movement were significant. The region was found to be below the participant's knee-cap.

We performed two experiments with the able-bodied participant and the SLS. The first was a weight shifting experiment during which the participant was asked to shift their body weight from one leg to the other (see Figure 3d) while standing on a split-belt treadmill (1000Hz, Bertec Corp., USA) to measure the corresponding vertical ground reaction force (GRF). In the following dynamic walking experiment, the participant walked on the split-belt treadmill. During both experiments,

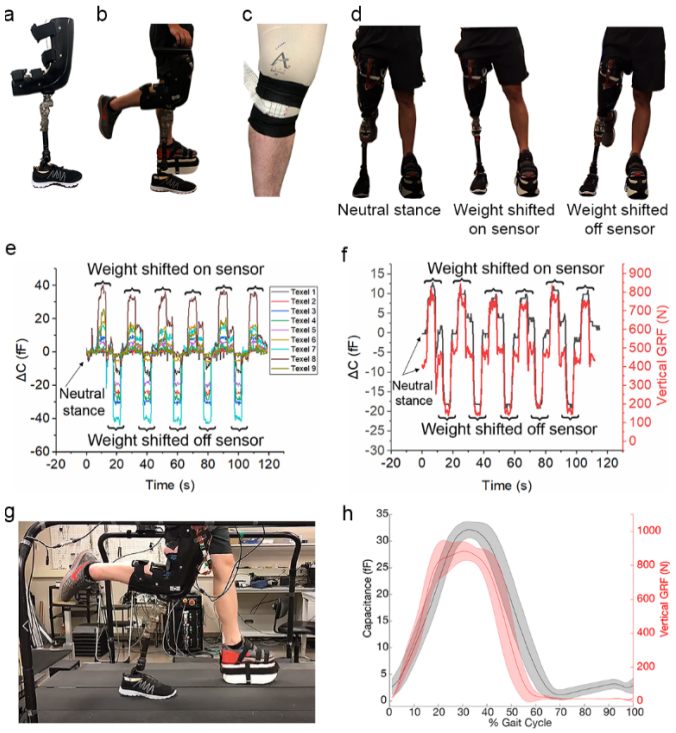

Fig. 3. Able-Bodied testing using a bent-knee adapter (a) Bent-knee adapter (b) Able-bodied participant wearing bent-knee adapter (c) Placement of SLS on the anterior location on top of the prosthetic liner (d) Weight shifting experiment - participant's stances (e) Change in capacitance of the nine texels during bodyweight shifting experiments (f) Average capacitance change during bodyweight shifting experiments. For the weight shifting experiments, the neutral stance was considered as the baseline and was removed from the general capacitance profile. (g) Dynamic walking experiment (h) Change in capacitance and GRF during walking experiments. For the walking experiments, the minimum capacitance value during the walking trials (i.e. while the bent-knee adapter was unloaded) was taken as the baseline and removed from the response.

a signal was used to synchronize the SLS output and the GRF recordings. The weight-shifting trials helped determine if the SLS sensor was capable of withstanding and detecting force changes induced by human body weight shifting. Walking trials allowed us to determine if the system and electronics were sufficiently durable to withstand dynamic activities while also applying repetitive force cycles to understand the repeatability of the sensors. Additionally, walking trials enabled the observation of whether the sensors were capable of detecting changes in force during transient activities. The participant's limb was in contact with a ground pad connected to the circuit to standardize the shunting of the limb and to provide external electric field shielding. The sensors were evaluated in-vitro on a benchtop after each experiment using the real-time data visualization to ensure no sensor damage occurred during the human experimentation.

The results from the weight shifting experiments for each texel are shown in Figure 3e. This demonstrates the ability of the SLS to collect individual capacitance values from each texel. The average response of the nine texels shown in Figure 3f provides a clear understanding of the change in capacitance when the participant shifted their body weight. GRF and ΔC follow similar trends indicating that the SLS is capable of tracking changes in weight-shifting movements.

During the weight shifting experiment, the participant was initially in a neutral stance and then shifted their body weight onto the SLS/bent-knee adapter which resulted in increased capacitance. The participant then returned to a neutral stance and subsequently shifted their body weight onto their other leg, resulting in a decrease in capacitance as pressure was removed from the sensor. We hypothesize that the observed variation in the sensor output at the neutral stance is due to the natural variation in human movement

In the subsequent walking trial, the able-bodied participant walked on the treadmill at a speed of 0.65 m/s (selected based on the subject's comfort level) for around one minute or approximately twenty walking cycles (see Figure 3g). Walking speeds vary for LL amputees with reported speeds including 0.60 [46] and 0.78 m/s [47] therefore, the walking speed used here is within a typical range. In post-processing, the GRF and SLS data were time-synced using a square-wave pulse (5 V) that was sent to each system at the start of the trial. To compare behavior across gait cycles, we segmented the data into individual gait cycles starting at each heel strike (20 N threshold). We then averaged the GRF and SLS data across all cycles (see Figure 3h). Overall, the SLS provided consistent capacitive readings with little variation during the walking experiment. In general, the SLS response (ΔC) followed the GRF output, indicating that our sensor tracked the pressure variation at its location corresponding to the changes in GRF during walking. During both the weight-shifting and walking experiments, the capacitance response was different for each texel, indicating a pressure distribution across the area.

The results of the able-bodied experiments show that the SLS is sufficiently robust to withstand its intended application. The SLS continued to function throughout the able-bodied experiments and provided consistent and meaningful data during multiple cycles of dynamic loading. Further, these results indicated that the sensors may be suitable for ISE pressure monitoring.

IV. Amputee Testing

In the final phase, the SLS was evaluated on a participant with bilateral transtibial amputations to determine if the sensors provide reliable qualitative data and are sufficiently durable to withstand the real dynamic ISE environment. Based on the able-body testing evaluation, we added additional conductive fabric layers to the SLS for electric field shielding before this experiment, to reduce electromagnetic interference and noise.

Two such shielded SLS arrays were placed on the participant's left residual limb in two anatomical regions of clinical interest [13], [22] where prosthetic sockets typically apply higher levels of pressure: the PT and PD (see Figure 2d and Figure 4a). We determined the pressure sensor placement based on the anatomical landmarks from the amputated limb [21], [22]. The SLSs were taped to the participant's liner before the participant donned their prosthetic socks. The participant reported that the SLS caused no additional discomfort during experimentation.

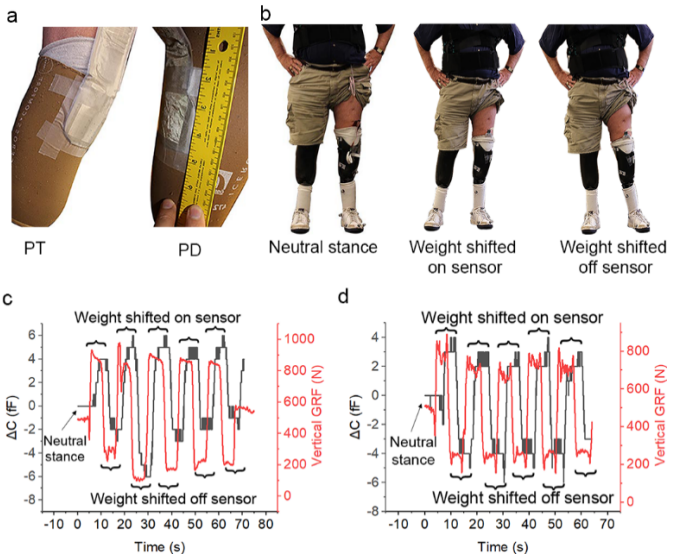

Fig. 4. Amputee testing (a) SLS placed at the PT and PD (b) Weight shifting - participant's stances. Average capacitance change during bodyweight shifting experiments at the (c) PT and (d) PD. For the weight shifting experiments, the neutral stance was considered as the baseline and was removed from the general capacitance profile.

Similar to the able-bodied experiment, the amputee was asked to complete two experimental procedures. The first was a weight shifting experiment during which the participant shifted their body weight from one leg to the other, as shown in Figure 4b while standing on the split-belt treadmill to measure the corresponding GRF. In the second experiment, the participant was asked to walk on the split-belt treadmill. During both experiments, a signal was used to synchronize the SLS output and GRF recordings. The experiments were designed to elucidate the same points made earlier in the case of the able-bodied experiment. The sensors were tested on the benchtop after each experiment using real-time data visualization to ensure no damage occurred by the amputee testing procedure.

The average SLS responses recorded during weight shifting experiments at the PT and PD are shown in Figures 4c and 4d respectively. The capacitive response was smoothed using an adjacent-averaging method. As we observed with the able-bodied testing, when the participant shifted body weight onto the leg with the SLS, the resulting capacitance increased. Alternatively, when the participant shifted body weight onto the other leg and off-loaded the sensor, the capacitance decreased. The peak ΔC values were in similar ranges regardless of anatomical location however, slightly larger at the PT. Higher pressures are anticipated at this location with several studies in the literature reporting peak ISE pressures at the PT [11], [28], [48]. This can be attributed to common socket designs that aim to distribute the majority of an amputee's body weight on the PT [48]. During amputee testing, a time lag was observed between the GRF and ΔC peaks at both anatomical locations which were not observed during able-bodied trials. This can be explained by the placement of the sensors and the fact that GRF was measured by the treadmill beneath the participant's foot. In able-bodied testing,

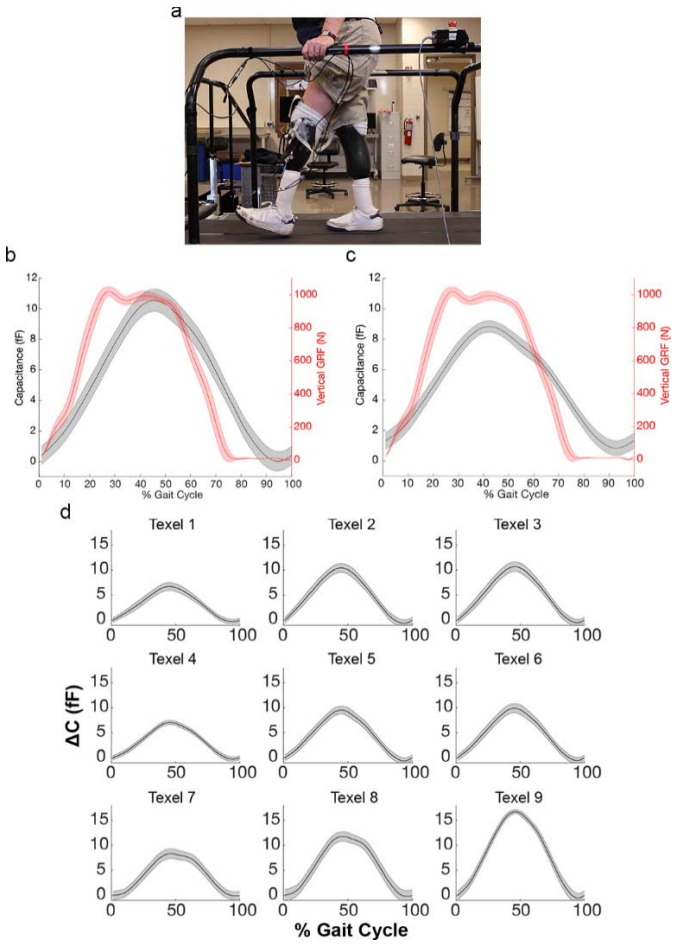

Fig. 5. Amputee testing results (a) Participant walking on a treadmill. The average change in capacitance and GRF at the (b) PT and (c) PD (d) Response of individual texels at the PT during walking. For the walking experiments, the minimum capacitance (i.e. while the prosthesis was unloaded) was taken as the baseline and removed from the capacitance response.

the sensor was placed beneath the participant's bent-knee, parallel to the treadmill belt, therefore it experienced a similar load profile at a similar time as the bottom of the foot. In contrast, during amputee trials, the sensors were placed around the residual limb, not parallel to the treadmill belt. As a result, it experienced a load profile different than that measured by the treadmill, thereby experiencing peak loading at a different time.

During the subsequent walking trials shown in Figure 5a, the participant walked on the treadmill at a speed of 0.41 m/s (selected based on the subject's comfort level) for around one minute or approximately twenty walking cycles. While this walking speed is slightly lower than reported values for LL amputees (0.60 [46] and 0.78 m/s [47]) this may be explained by the fact that the subject in this experiment was a bilateral amputee who may experience additional challenges during walking. We completed post-processing (alignment, segmentation, and averaging) for the GRF and capacitance data of this walking trial in a similar way to able-bodied experiments described previously. The results of the walking trials, presented for the PT and PD in Figure 5b and 5c, provide expected trends with maximum GRFs/SLS values measured during the stance phase (initial 60% of the gait cycle) [49] and minimum GRF/SLS response measured during swing phase (final 40% of the gait cycle) [49]–[52]. Additionally, the SLS response provided little variation during the walking experiment. As noted earlier for the weight-shifting trials, the time lag between the peak GRF and ΔC values can be attributed to the placement of the sensors relative to the location of the GRF measurement. Additionally, a larger value was observed at the PT than the PD. As previously mentioned, peak pressures are expected at the PT [11], [28], [48] and the PT is often the main site of weight-bearing during ambulation [53]. While verifying the source of these differences requires a further analysis which we reserve for a future study, the socket fit is likely to have contributed. During both the weight-shifting and walking experiments, the capacitance response was different for each texel, as shown in Figure 5d, indicating a pressure distribution across the area.

V. Conclusion

In this work, we presented a new method to seamlessly monitor pressure within the ISE utilizing a simple and inexpensive textile-based, soft sensor system. We described in detail the SLS system including textile interconnects, high-speed data recording, and transmission from four sensor arrays which require little power enabling up to twelve hours of data collection. Further, we presented two experimental approaches to systematically incorporate SLS within a simulated in-vitro and in-vivo ISE environment before evaluation with an amputee subject. In the first experiment, the SLS provided sound pressure tracking results for proof-of-concept when placed on the curved surface of the artificial limb. The sensor system continued to collect reliable information from multiple sensor arrays simultaneously throughout the experiment. The results of the subsequent able-bodied experiments show that the SLS was sufficiently robust to withstand human testing. The SLS continued to function throughout the able-bodied experiments and provided consistent data during cycles of dynamic loading which could be qualitatively explained by the general movement of the able-bodied participant. Results of the amputee participant experiment indicated that the SLS is robust and can monitor the ISE without causing discomfort to the subject. The results also correspond well to the general movement of the amputee participant. In summary, these preliminary results validate the concept of SLS as a promising approach for monitoring pressure distribution within the ISE that is amenable to full integration into prosthetic components. The future work will involve expansion to a larger clinical study with additional subjects, calibration of the sensors for the assessment of absolute pressure values, as well as a study of the effect of use, aging and washing on the material and sensor performance.

Acknowledgment

The authors would like to acknowledge the Nonwovens Institute at NC State University for providing the nonwoven fabric for this research. They would also like to acknowledge and thank Derek Frankena, CPO for the fabrication of the artificial limb.

REFERENCES

[1] K. Ziegler-Graham, E. J. MacKenzie, P. L. Ephraim, T. G. Travison, and R. Brookmeyer, "Estimating the prevalence of limb loss in the United States: 2005 to 2050," *Arch. Phys. Med. Rehabil.*, vol. 89, no. 3, pp. 422–429, Mar. 2008, doi: 10.1016/j.apmr.2007.11.005.

[2] T. L. Beil, G. M. Street, and S. J. Covey, "Interface pressures during ambulation using suction and vacuum-assisted prosthetic sockets," *J. Rehabil. Res. Develop.*, vol. 39, no. 6, pp. 693–700, 2002.

[3] T. R. Dillingham, L. E. Pezzin, E. J. MacKenzie, and A. R. Burgess, "Use and satisfaction with prosthetic devices among persons with trauma-related amputations: A long-term outcome study," *Amer. J. Phys. Med. Rehabil.*, vol. 80, no. 8, pp. 563–571, Aug. 2001, doi: 10.1097/00002060-200108000-00003.

[4] C. C. Nielsen, "A survey of amputees: Functional level and life satisfaction, information needs, and the prosthetist's role," *J. Prosthetics Orthotics*, vol. 3, no. 3, pp. 125–129, 1991, doi: 10.1097/00008526-199106000-00009.

[5] D. M. Sengeh and H. Herr, "A variable-impedance prosthetic socket for a transtibial amputee designed from magnetic resonance imaging data," *J. Prosthetics Orthotics*, vol. 25, no. 3, pp. 129–137, Jul. 2013, doi: 10.1097/JPO.0b013e31829be19c.

[6] P. Laszczak, L. Jiang, D. L. Bader, D. Moser, and S. Zahedi, "Development and validation of a 3D-printed interfacial stress sensor for prosthetic applications," *Med. Eng. Phys.*, vol. 37, no. 1, pp. 132–137, Jan. 2015, doi: 10.1016/j.medengphy.2014.10.002.

[7] S. Ali, N. A. A. Osman, A. Eshraghi, H. Gholizadeh, N. A. B. A. Razak, and W. A. B. B. W. Abas, "Interface pressure in transtibial socket during ascent and descent on stairs and its effect on patient satisfaction," *Clin. Biomech.*, vol. 28, nos. 9–10, pp. 994–999, Nov. 2013, doi: 10.1016/j.clinbiomech.2013.09.004.

[8] H. E. Meulenbelt, J. H. Geertzen, M. F. Jonkman, and P. U. Dijkstra, "Determinants of skin problems of the stump in lower-limb amputees," *Arch. Phys. Med. Rehabil.*, vol. 90, no. 1, pp. 74–81, Jan. 2009, doi: 10.1016/j.apmr.2008.07.015.

[9] P. Sewell, S. Noroozi, J. Vinney, and S. Andrews, "Developments in the trans-tibial prosthetic socket fitting process: A review of past and present research," *Prosthetics Orthotics Int.*, vol. 24, no. 2, pp. 97–107, 2000, doi: 10.1080/03093640008726532.

[10] J. E. Sanders, D. Lain, A. J. Dralle, and R. Okumura, "Interface pressures and shear stresses at thirteen socket sites on two persons with transtibial amputation," *J. Rehabil. Res. Develop.*, vol. 34, no. 1, pp. 19–43, Jan. 1997.

[11] J. R. Pearson *et al.*, "Pressures in critical regions of the below-knee patellar-tendon-bearing prosthesis," *Bull. Prosthetics Res.*, vol. 10, no. 19, p. 52, 1973.

[12] J. E. Sanders, C. H. Daly, and E. M. Burgess, "Interface shear stresses during ambulation with a below-knee prosthetic limb," *J. Rehabil. Res. Develop.*, vol. 29, no. 4, p. 1, 1992, doi: 10.1682/JRRD.1992.10.0001.

[13] J. W. Rae and J. L. Cockrell, "Interface pressure and stress distribution in prosthetic fitting," *Bull. Prosthetics Res.*, vol. 10, no. 15, pp. 64–111, 1971.

[14] E. Al-Fakih, N. A. Osman, and F. M. Adikan, "Techniques for interface stress measurements within prosthetic sockets of transtibial amputees: A review of the past 50 years of research," *Sensors*, vol. 16, no. 7, p. 1119, Jul. 2016, doi: 10.3390/s16071119.

[15] N. A. A. Osman, W. D. Spence, S. E. Solomonidis, J. P. Paul, and A. M. Weir, "Transducers for the determination of the pressure and shear stress distribution at the stump—Socket interface of trans-tibial amputees," *Proc. Inst. Mech. Eng., B, J. Eng. Manuf.*, vol. 224, no. 8, pp. 1239–1250, Aug. 2010, doi: 10.1243/09544054JEM1820.

[16] J. E. Sanders and C. H. Daly, "Normal and shear stresses on a residual limb in a prosthetic socket during ambulation: Comparison of finite element results with experimental measurements," *J. Rehabil. Res. Develop.*, vol. 30, no. 2, p. 191, 1993.

[17] M. Silver-Thorn, J. W. Steege, and D. S. Childress, "A review of prosthetic interface stress investigations," *J. Rehabil. Res. Develop.*, vol. 33, no. 3, pp. 253–266, 1996.

[18] C. H. Y. Lai and C. W. P. Li-Tsang, "Validation of the Pliance X system in measuring interface pressure generated by pressure garment," *Burns*, vol. 35, no. 6, pp. 845–851, Sep. 2009, doi: 10.1016/j.burns.2008.09.013.

[19] P. Saccomandi, E. Schena, C. Oddo, L. Zollo, S. Silvestri, and E. Guglielmelli, "Microfabricated tactile sensors for biomedical applications: A review," *Biosensors*, vol. 4, no. 4, pp. 422–448, Nov. 2014.

[20] C.-Y. Ko *et al.*, "Development of a sensor to measure stump/socket interfacial shear stresses in a lower-extremity amputee," *Int. J. Precis. Eng. Manuf.*, vol. 19, no. 6, pp. 899–905, Jun. 2018, doi: 10.1007/s12541-018-0106-z.

[21] S. I. Wolf, M. Alimusaj, L. Fradet, J. Siegel, and F. Braatz, "Pressure characteristics at the stump/socket interface in transtibial amputees using an adaptive prosthetic foot," *Clin. Biomech.*, vol. 24, no. 10, pp. 860–865, Dec. 2009, doi: 10.1016/j.clinbiomech.2009.08.007.

[22] P. Dou, X. Jia, S. Suo, R. Wang, and M. Zhang, "Pressure distribution at the stump/socket interface in transtibial amputees during walking on stairs, slope and non-flat road," *Clin. Biomech.*, vol. 21, no. 10, pp. 1067–1073, Dec. 2006, doi: 10.1016/j.clinbiomech.2006.06.004.

[23] A. Eshraghi, N. A. A. Osman, H. Gholizadeh, S. Ali, and W. A. B. W. Abas, "Interface stress in socket/residual limb with transtibial prosthetic suspension systems during locomotion on slopes and stairs," *Amer. J. Phys. Med. Rehabil.*, vol. 94, no. 1, pp. 1–10, Jan. 2015, doi: 10.1097/PHM.0000000000000134.

[24] J. W. Wheeler *et al.*, "MEMS-based bubble pressure sensor for prosthetic socket interface pressure measurement," in *Proc. Annu. Int. Conf. IEEE Eng. Med. Biol. Soc.*, Aug. 2011, pp. 2925–2928, doi: 10.1109/IEMBS.2011.6090805.

[25] E. C. Swanson, J. B. McLean, K. J. Allyn, C. B. Redd, and J. E. Sanders, "Instrumented socket inserts for sensing interaction at the limb-socket interface," *Med. Eng. Phys.*, vol. 51, pp. 111–118, Jan. 2018.

[26] P. Laszczak *et al.*, "A pressure and shear sensor system for stress measurement at lower limb residuum/socket interface," *Med. Eng. Phys.*, vol. 38, no. 7, pp. 695–700, Jul. 2016, doi: 10.1016/j.medengphy.2016.04.007.

[27] G. Sordo and L. Lorenzelli, "Design of a novel tri-axial force sensor for optimized design of prosthetic socket for lower limb amputees," in *Proc. Symp. Design, Test, Integr. Packag. MEMS/MOEMS (DTIP)*, May 2016, pp. 1–4.

[28] M. Zhang, A. R. Turner-Smith, A. Tanner, and V. C. Roberts, "Clinical investigation of the pressure and shear stress on the trans-tibial stump with a prosthesis," *Med. Eng. Phys.*, vol. 20, no. 3, pp. 188–198, Apr. 1998, doi: 10.1016/S1350-4533(98)00013-7.

[29] R. B. Williams, D. Porter, V. C. Roberts, and J. F. Regan, "Triaxial force transducer for investigating stresses at the stump/socket interface," *Med. Biol. Eng. Comput.*, vol. 30, no. 1, pp. 89–96, Jan. 1992, doi: 10.1007/BF02446199.

[30] S. Toyama *et al.*, "Development of wearable sheet-type shear force sensor and measurement system that is insusceptible to temperature and pressure," *Sensors*, vol. 17, no. 8, p. 1752, Jul. 2017, doi: 10.3390/s17081752.

[31] Z. Zhao *et al.*, "Machine-washable and breathable pressure sensors based on triboelectric nanogenerators enabled by textile technologies," *Nano Energy*, vol. 70, Apr. 2020, Art. no. 104528, doi: 10.1016/j.nanoen.2020.104528.

[32] J. Lee *et al.*, "Conductive fiber-based ultrasensitive textile pressure sensor for wearable electronics," *Adv. Mater.*, vol. 27, no. 15, pp. 2433–2439, Apr. 2015, doi: 10.1002/adma.201500009.

[33] O. Atalay, A. Atalay, J. Gafford, and C. Walsh, "A highly sensitive capacitive-based soft pressure sensor based on a conductive fabric and a microporous dielectric layer," *Adv. Mater. Technol.*, vol. 3, no. 1, Jan. 2018, Art. no. 1700237, doi: 10.1002/admt.201700237.

[34] C. Choi, J. M. Lee, S. H. Kim, S. J. Kim, J. Di, and R. H. Baughman, "Twistable and stretchable sandwich structured fiber for wearable sensors and supercapacitors," *Nano Lett.*, vol. 16, no. 12, pp. 7677–7684, Dec. 2016, doi: 10.1021/acs.nanolett.6b03739.

[35] C. Wang *et al.*, "Carbonized silk fabric for ultrastretchable, highly sensitive, and wearable strain sensors," *Adv. Mater.*, vol. 28, no. 31, pp. 6640–6648, Aug. 2016, doi: 10.1002/adma.201601572.

[36] J. Hong, Z. Pan, Z. Wang, M. Yao, J. Chen, and Y. Zhang, "A large-strain weft-knitted sensor fabricated by conductive UHMWPE/PANI composite yarns," *Sens. Actuators A, Phys.*, vol. 238, pp. 307–316, Feb. 2016, doi: 10.1016/j.sna.2015.12.028.

[37] A. Frutiger *et al.*, "Capacitive soft strain sensors via multicore-shell fiber printing," *Adv. Mater.*, vol. 27, no. 15, pp. 2440–2446, Apr. 2015, doi: 10.1002/adma.201500072.

[38] T. Agcayazi, M. McKnight, H. Kausche, T. Ghosh, and A. Bozkurt, "A finger touch force detection method for textile based capacitive tactile sensor arrays," in *Proc. IEEE SENSORS*, Oct. 2016, pp. 1–3, doi: 10.1109/ICSENS.2016.7808528.

[39] M. McKnight, T. Agcayazi, H. Kausche, T. Ghosh, and A. Bozkurt, "Sensing textile seam-line for wearable multimodal physiological monitoring," in *Proc. 38th Annu. Int. Conf. IEEE Eng. Med. Biol. Soc. (EMBC)*, Aug. 2016, pp. 311–314, doi: 10.1109/EMBC.2016.7590702.

[40] R. White, M. McKnight, J. Tabor, T. Ghosh, T. Agcayazi, and A. Bozkurt, "A wetness detection technique towards scalable, array-based, fully-textile sensing," in *Proc. IEEE Biomed. Circuits Syst. Conf. (BioCAS)*, Oct. 2018, pp. 1–4.
[41] T. Agcayazi, J. Tabor, M. McKnight, I. Martin, T. K. Ghosh, and A. Bozkurt, "Fully-textile seam-line sensors for facile textile integration and tunable multi-modal sensing of pressure, humidity, and wetness," *Adv. Mater. Technol.*, vol. 5, no. 8, 2020, Art. no. 2000155, doi: 10.1002/admt.202000155.
[42] M. N. Orlin and T. G. McPoil, "Plantar pressure assessment," *Phys. Therapy*, vol. 80, no. 4, pp. 399–409, Apr. 2000, doi: 10.1093/ptj/80.4.399.
[43] M. M. Wernke, R. M. Schroeder, M. L. Haynes, L. L. Nolt, A. W. Albury, and J. M. Colvin, "Progress toward optimizing prosthetic socket fit and suspension using elevated vacuum to promote residual limb health," *Adv. Wound Care*, vol. 6, no. 7, pp. 233–239, Jul. 2017, doi: 10.1089/wound.2016.0719.
[44] D. Quintero, D. J. Villarreal, and R. D. Gregg, "Preliminary experiments with a unified controller for a powered knee-ankle prosthetic leg across walking speeds," in *Proc. IEEE/RSJ Int. Conf. Intell. Robots Syst. (IROS)*, Oct. 2016, pp. 5427–5433.
[45] F. Sup, H. A. Varol, J. Mitchell, T. Withrow, and M. Goldfarb, "Design and control of an active electrical knee and ankle prosthesis," in *Proc. 2nd IEEE RAS EMBS Int. Conf. Biomed. Robot. Biomechtron.*, Oct. 2008, pp. 523–528.
[46] C. R. C. Walker, R. R. Ingram, M. G. Hullin, and S. W. McCreath, "Lower limb amputation following injury: A survey of long-term functional outcome," *Injury*, vol. 25, no. 6, pp. 387–392, Aug. 1994, doi: 10.1016/0020-1383(94)90132-5.
[47] M. E. Jones, G. M. Bashford, and J. M. Mann, "Weight bearing and velocity in trans-tibial and trans-femoral amputees," *Prosthetics Orthotics Int.*, vol. 21, no. 3, pp. 183–186, Dec. 1997, doi: 10.3109/03093649709164553.
[48] N. A. A. Osman, W. D. Spence, S. E. Solomonidis, J. P. Paul, and A. M. Weir, "The patellar tendon bar! Is it a necessary feature?" *Med. Eng. Phys.*, vol. 32, no. 7, pp. 760–765, Sep. 2010, doi: 10.1016/j.medengphy.2010.04.020.
[49] J. B. Webster and B. J. Darter, "Principles of normal and pathologic gait," in *Atlas of Orthoses and Assistive Devices*, 5th ed. Amsterdam, The Netherlands: Elsevier, 2019, pp. 49–62.
[50] D. H. K. Chow, A. D. Holmes, C. K. L. Lee, and S. W. Sin, "The effect of prosthesis alignment on the symmetry of gait in subjects with unilateral transtibial amputation," *Prosthetics Orthotics Int.*, vol. 30, no. 2, pp. 114–128, Aug. 2006, doi: 10.1080/03093640600568617.
[51] A. L. Lenz and T. R. Bush, "Evaluating shear and normal force with the use of an instrumented transtibial socket: A case study," *Med. Eng. Phys.*, vol. 71, pp. 102–107, Sep. 2019, doi: 10.1016/j.medengphy.2019.07.002.
[52] A. Eshraghi, N. A. A. Osman, H. Gholizadeh, S. Ali, S. K. Sævarsson, and W. A. B. W. Abas, "An experimental study of the interface pressure profile during level walking of a new suspension system for lower limb amputees," *Clin. Biomech.*, vol. 28, no. 1, pp. 55–60, Jan. 2013.
[53] H. Gholizadeh, N. A. A. Osman, A. Eshraghi, N. Arifin, and T. Y. Chung, "A comparison of pressure distributions between two types of sockets in a bulbous stump," *Prosthetics Orthotics Int.*, vol. 40, no. 4, pp. 509–516, Aug. 2016, doi: 10.1177/0309364614564022.

Jordan Tabor received the M.S. degree in textile engineering from North Carolina (NC) State University, where she is currently pursuing the Ph.D. degree in fiber and polymer science. Her research interests are cross-functional including topics such as technical textiles and adaptive and responsive textiles. Her current research focuses on designing and fabricating wearable, textile-based sensors for biomedical applications, specifically prosthetics.

Talha Agcayazi received the B.Sc. degree from George Mason University in 2015 and the Ph.D. degree from North Carolina (NC) State University in 2020. During his graduate degree, he worked on three main research areas: flexible physical sensors (pressure, shear, and strain), physiological sensors (bio-impedance, ExG, and biochemistry), and robotics (embedded systems and machine learning). His Ph.D. dissertation was on attachment quality monitoring of prosthetic limbs with flexible textile sensors. He is currently a Research Engineer with Facebook Reality Labs.

Aaron Fleming received the B.S. degree in mechanical engineering with North Carolina (NC) State University, Raleigh, NC, USA. He is currently pursuing the Ph.D. degree with the UNC/NC State Joint Department of Biomedical Engineering, University of North Carolina at Chapel Hill, and also with the North Carolina State University. He is also a NIH Predoctoral Fellow (F31) with the Eunice Kennedy Shriver National Institute, Child Health and Human Development. His research interests include the development of neural control of lower limb prostheses, and improving access to orthotic and prosthetic devices for individuals in low-resource settings.

Brendan Thompson received the B.S. degree in electrical engineering from North Carolina (NC) State University in 2020. In 2021, he joined the Electrical Engineering Ph.D. Program, NC State University, where he is currently a Research Assistant with the Integrated Bionic Microsystems Lab.

Ashish Kapoor received the master's degree in textile engineering from IIT Delhi, India, in 2015. In August 2015, he joined the Fiber and Polymer Science Ph.D. Program at Wilson College of Textiles, North Carolina (NC) State University, and started working under the direction of Dr. Tushar K. Ghosh in the field of electronic textiles, where he worked toward the development of fiber-based multimodal and multifunctional active sensory textiles. He received the NC State University's Provost Doctoral Recruitment Fellowship from 2015 to 2016, DAAD (German Academic Exchange Service) RISE Professional Scholarship in 2018 and NC State University's Graduate School Summer Fellowship in 2019. Since the completion of his Ph.D. in March 2020, he has been a Technology Development Etch Module Engineer with Intel, Hillsboro, OR, USA.

Ming Liu (Member, IEEE) received the B.S. and M.S. degrees in mechatronics from the Beijing Institute of Technology and the Ph.D. degree in mechanical engineering from the University of Rhode Island. He is currently a Research Assistant Professor with the UNC/NC State Joint Department of Biomedical Engineering, University of North Carolina at Chapel Hill, and also with the North Carolina State University. His research interests include amputee rehabilitation, prosthesis design and control, and time series analysis.

Michael Y. Lee received the medical degree from the University of Illinois College of Medicine, the residency degree from the Rehabilitation Institute of Chicago, Northwestern University, and the master's degree in health administration from The University of North Carolina at Chapel Hill. He was the Chair of the H. Ben Taub Department of Physical Medicine and Rehabilitation, Baylor College of Medicine in August 2019. Before joining the Baylor College of Medicine, he was the Sidna C. Rizzo Distinguished Professor and the Founding Chair of the Department of Physical Medicine and Rehabilitation, University of North Carolina at Chapel Hill for more than 23 years. While there, he led the design and launch of UNC Hospitals Inpatient Rehabilitation Center, Center for Rehabilitation Care (an Outpatient rehabilitation Center), and UNC Hospitals Imaging and Spine Center, a unique regional resource lauded for its comprehensive, multidisciplinary approach to spine disease diagnosis and treatment. His experience in establishing these centers and clinical programs, development of educational programs including a residency program, and nationally renowned research programs have contributed significantly to the further development of H. Ben Taub Department of Physical Medicine and Rehabilitation, Baylor College of Medicine.

He (Helen) Huang (Senior Member, IEEE) is currently the Jackson Family Distinguished Professor with the UNC/NC State Joint Department of Biomedical Engineering, University of North Carolina at Chapel Hill, and also with the North Carolina State University, and also with the Director of the Closed-Loop Engineering for Advanced Rehabilitation (CLEAR) core. Her research interests include neural-machine interfaces for prostheses and exoskeletons, human–robot interaction, adaptive and optimal control of wearable robots, and human movement control. She was a recipient of the Delsys Prize for Innovation in Electromyography, the Mary E. Switzer Fellowship with NIDRR, and the NSF CAREER Award. Her research has been sponsored by NSF, NIH, DOD, NIDRR (NIDILRR), and DARPA. She is a member of the Society for Neuroscience, AAAS, BMES, and ASB.

Alper Bozkurt (Senior Member, IEEE) received the master's degree in biomedical engineering from Drexel University, Philadelphia, PA, USA, and the Ph.D. degree from Cornell University, Ithaca, NY, USA. He is currently the Founder and the Director of the Integrated Bionic MicroSystems Laboratory and also a Professor with the Department of Electrical and Computer Engineering, North Carolina (NC) State University. He was a recipient of the Calhoun Fellowship from Drexel University, the Donald Kerr Award from Cornell University, the Chancellor's Innovation Award, the William F. Lane Outstanding Teacher Award and University Scholar Award from NC State University, the National Science Foundation CAREER Award, the IBM Faculty Award, and was included in the Popular Science Magazine 2015 Brilliant 10 list.

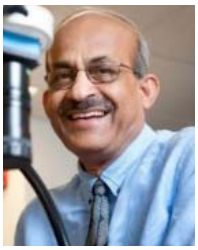

Tushar K. Ghosh (Member, IEEE) is currently the Klopman Distinguished Professor of Textiles with the Textile Engineering, Chemistry, and Science Department, North Carolina (NC) State University. He has been engaged in teaching and research in the area of fiber and polymer science in an academic environment for more than 30 years. His research interests include the mechanics of fibrous structures, characterization, and applications of fiber materials in technical applications, electronic textiles, and electroactive polymers. A continuing underlying focus of Dr. Ghosh's research has been to improve the current understanding of functional applications of fibers & textiles. His current research interests include the fabrication of sensors and actuators involving polymer nanocomposites, electroactive polymers, artificial muscle, and bio-inspired devices.